Supporting Information

Chirality Affects Aggregation Kinetics of Single-Walled Carbon Nanotubes

[1]IFTHEKER A KHAN, [1]ARM NABIUL AFROOZ, [1]JOSEPH R V FLORA, [2]P ARIETTE SCHIERZ, [3]P LEE FERGUSON, [4]TARA SABO-ATTWOOD, AND *[1]NAVID B SALEH

[1]Department of Civil and Environmental Engineering, University of South Carolina, Columbia, SC 29208

Department of Civil, Architectural, and Environmental Engineering, University of Texas, Austin, TX 78712

[3]Department of Civil and Environmental Engineering, Duke University, Durham, NC 27708

[4]Department of Environmental and Global Health, University of Florida, Gainesville, FL 32610

* Corresponding author: Navid B. Saleh, Email: salehn@engr.sc.edu, Phone: (803) 777-2288.

S1. Method for Aggregation Kinetics Experiment

For the TRDLS experiments, 2 mL of solution containing ~1 mg/L SWNT aqueous suspensions was added to pre-cleaned disposable borosilicate glass vials (Fisher Scientific, Pittsburg, PA); that were soaked in 2% cleaning solution (Extran MA01, EMD Chemicals, Gibbstown, NJ), and thoroughly rinsed with deionized water and oven dried (Fisher Scientific, Pittsburg, PA) under dust free conditions (*1*-*3*). Salt solutions were added to initiate aggregation and laser was directed to the sample immediately after the vial insertion to the toluene filled refractive index matched chamber. The scattered light intensity was detected at 90° by a photon counting module operating at 1.2 amperes and 5 volts (Perkin Elmer, Dumberry, Canada). The hydrodynamic radii of the particle clusters were determined through second-order cumulant analysis (ALV software) and average particle cluster size (R_0) was calculated in every 15 s corrected by auto correlation function for at least 30 min for each condition.

S2. Method for *ab initio* Calculations

The initial geometry of a repeating unit of an SG65 and SG76 SWNT molecule were obtained from visual molecular dynamics (VMD) (*4*). The ends of the SWNTs were terminated with hydrogen atoms; while the resulting molecular structures used in simulation were $C_{364}H_{22}$ and $C_{508}H_{26}$ for SG65 and SG76, respectively. The coordinates of each SWNT molecule were optimized (*5*) with dispersion corrected Density Functional Theory (DFT-D3) (*6*-*7*) using with the BLYP functional and the 6-31G basis set, implemented through TeraChem (*8*). The optimized SWNT molecule was re-oriented to its principal axis configuration using MacMolPlt (*9*); while a rigid-molecule potential energy surface scan was performed with the second SWNT molecule oriented 90º from the first and rotated 180º degrees along its longitudinal axis (Figure S1).

TABLE S1. Chiral angles and diameters for major and minor chiralities present in SG65 and SG76 SWNTs. ‘X’ symbol denotes presence of the chirality in respective sample

Chirality	**Diameter (nm)**	**Chiral Angle (degree)**	**SG65**	**SG76**
(6, 5)	0.756	27.0	X	X
(7,3)	0.704	17.1	X	
(7, 5)	0.827	24.5	X	X
(7, 6)	0.893	27.5		X
(8, 4)	0.838	19.1	X	
(9, 4)	0.914	17.5		X
(10,3)	0.934	12.8		X
(12,1)	0.993	3.6		X

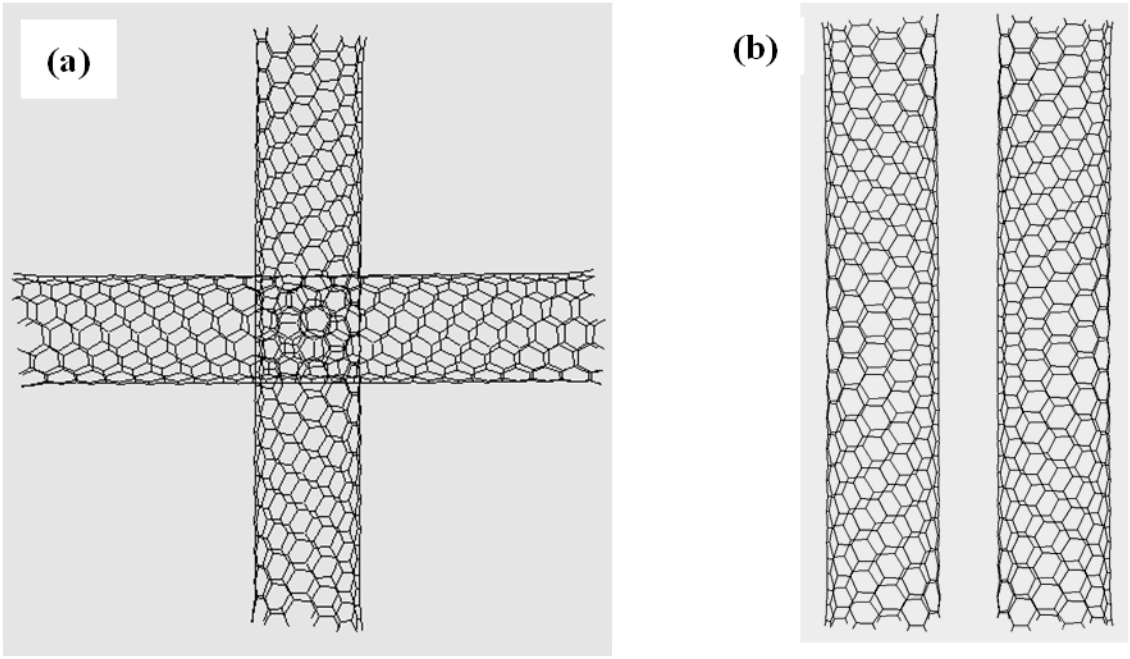

FIGURE S1. Orientation of the SG76 pair during a surface scan for rigid-molecule potential energy (a) perpendicular and (b) parallel.

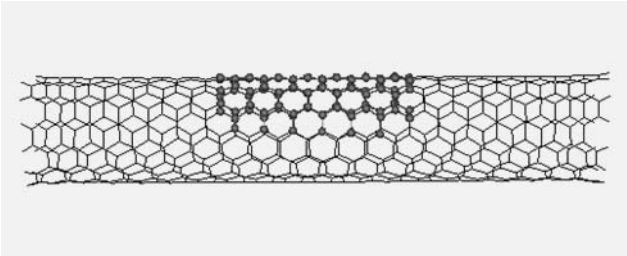

FIGURE S2. SG76 showing half of the middle third section that was run with 6-31+G(d) basis set, while the remaining atoms were run with a 6-31G basis set.

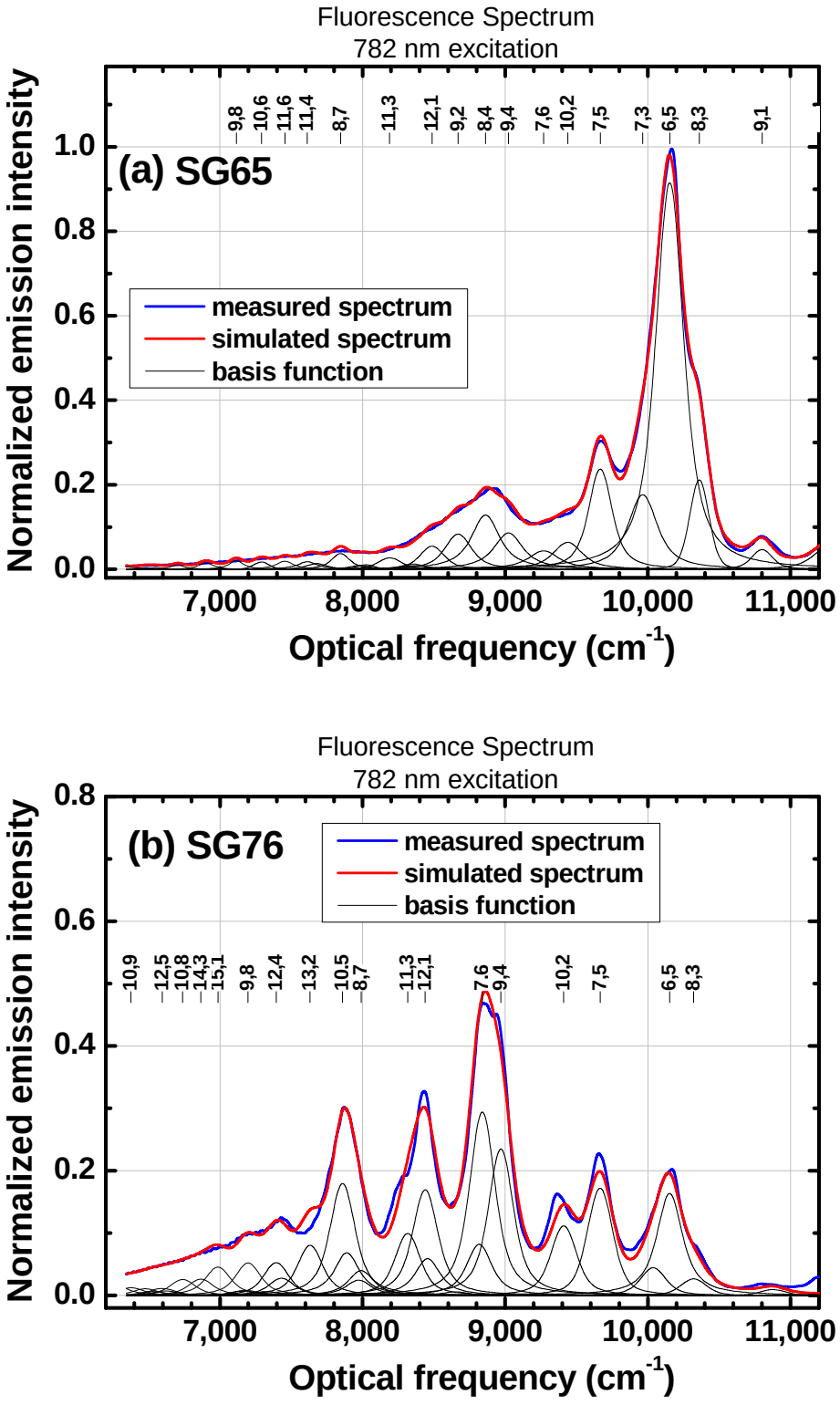

FIGURE S3. Fluorescence absorbance spectra of (a) SG65 (b) SG76 SWNTs. The measurements were performed at 782 nm excitation.

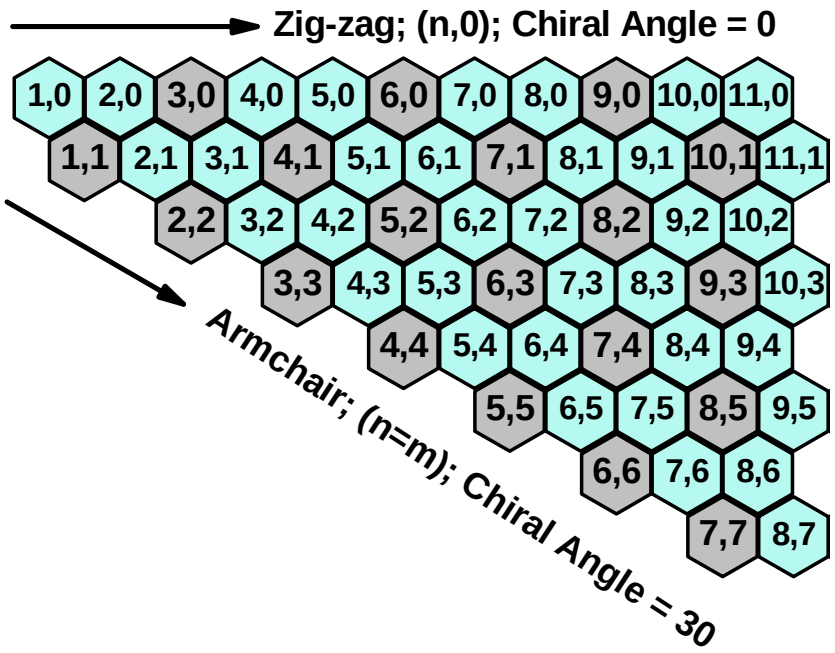

FIGURE S4. Chirality chart of SWNTs showing semiconducting (blue hexagons) and metallic (grey hexagons) chiral indices through color coding. The two arrows represent boundaries of atomic arrangements; horizontal arrow is the zig-zag and angular arrow is the armchair extreme for chiral arrangements.

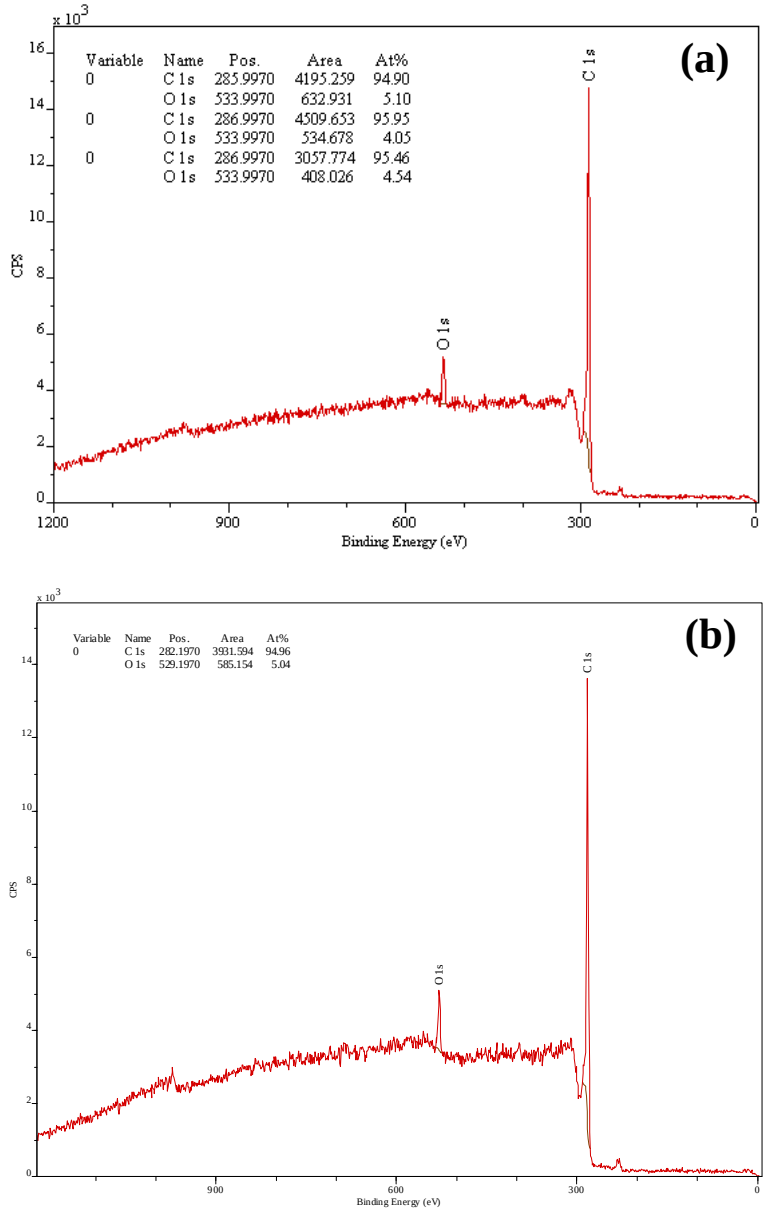

FIGURE S5. XPS spectra showing C1s and O1s peaks for pristine (a) SG65 and (b) SG76 SWNTs.

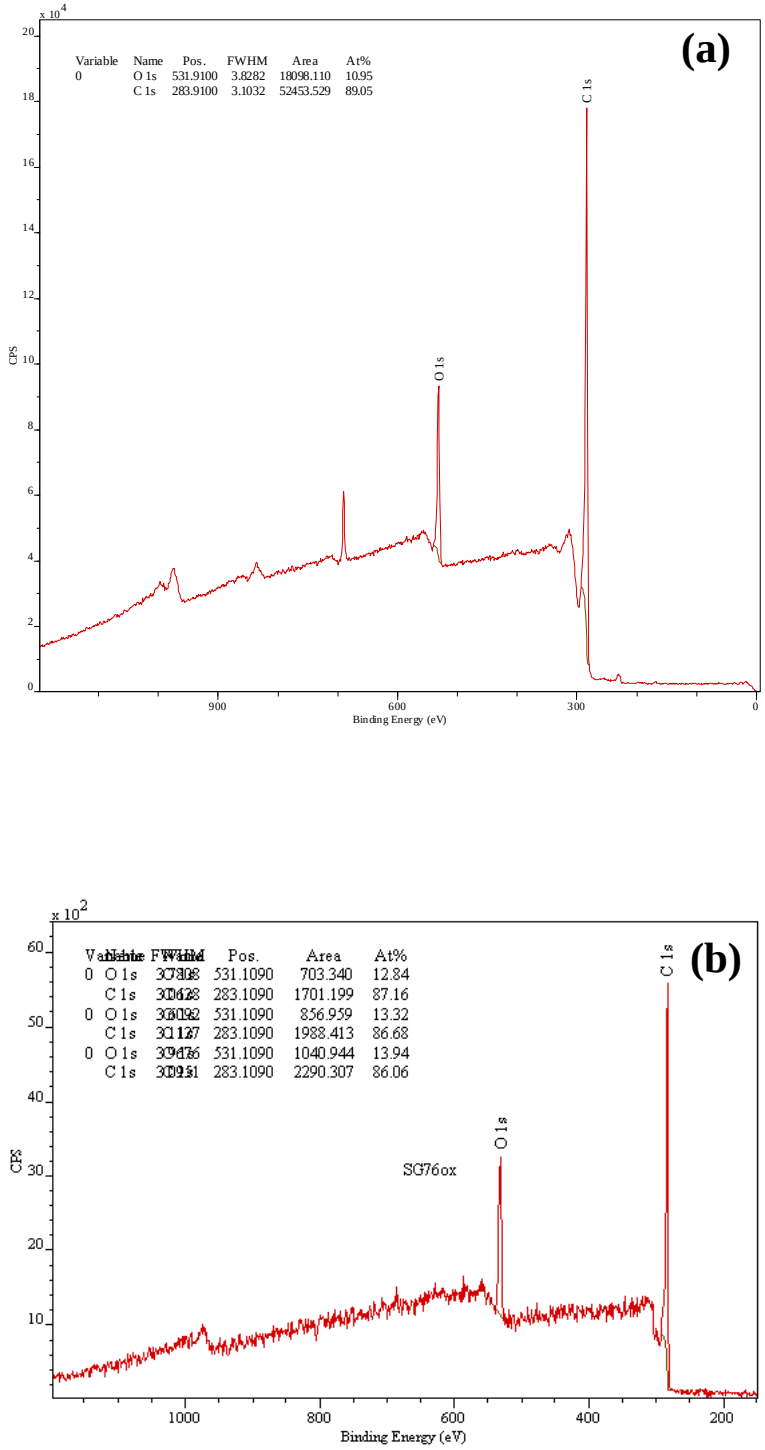

FIGURE S6. XPS spectra showing C1s and O1s peaks for functionalized (a) SG65 and (b) SG76 SWNTs.

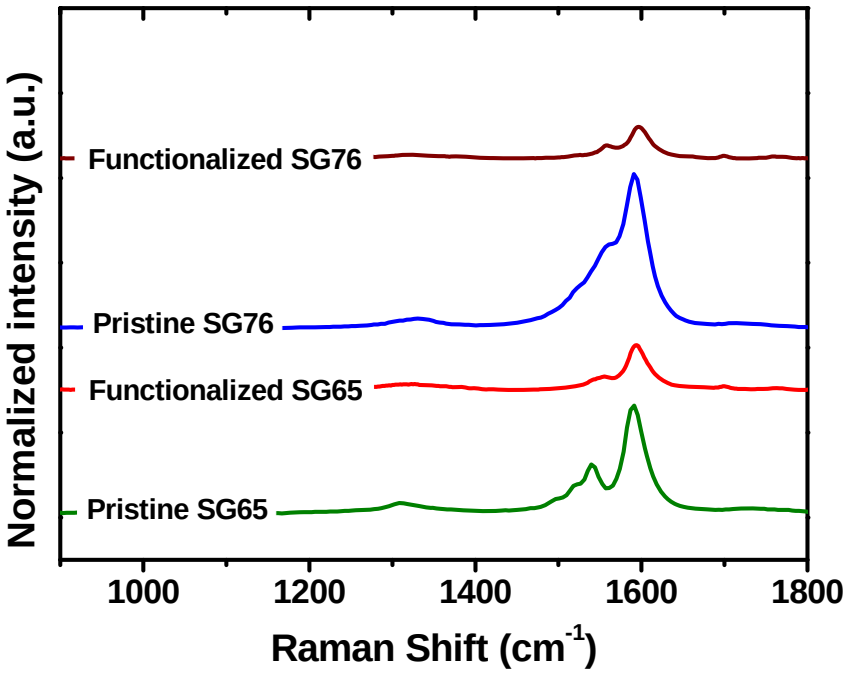

FIGURE S7. Raman spectra of pristine and oxidized SWNTs presenting the higher Raman frequency regions with defect representing 'D' band (near 1320 cm^{-1}) and graphitic signature containing 'G' band (near 1590 cm^{-1}). Intensity for each spectrum is relevant to that specific measurement and shows relative D/G intensities for that specific case.

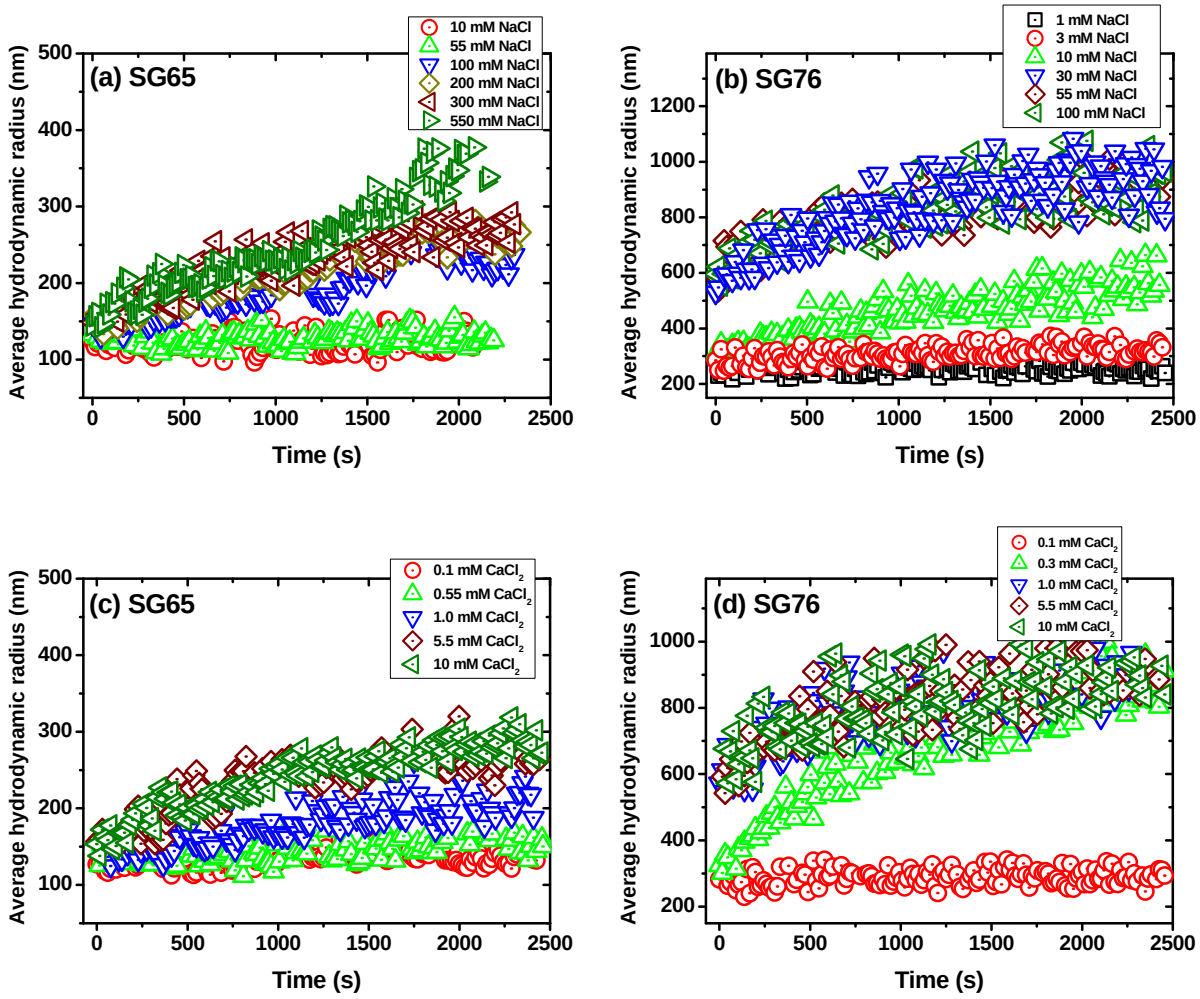

FIGURE S8. Aggregation profile of functionalized SWNTs in presence of (a-b) NaCl and (c-d) $CaCl_2$ salt. Measurements were carried out at pH of ~6.5 and a temperature of 20 °C.

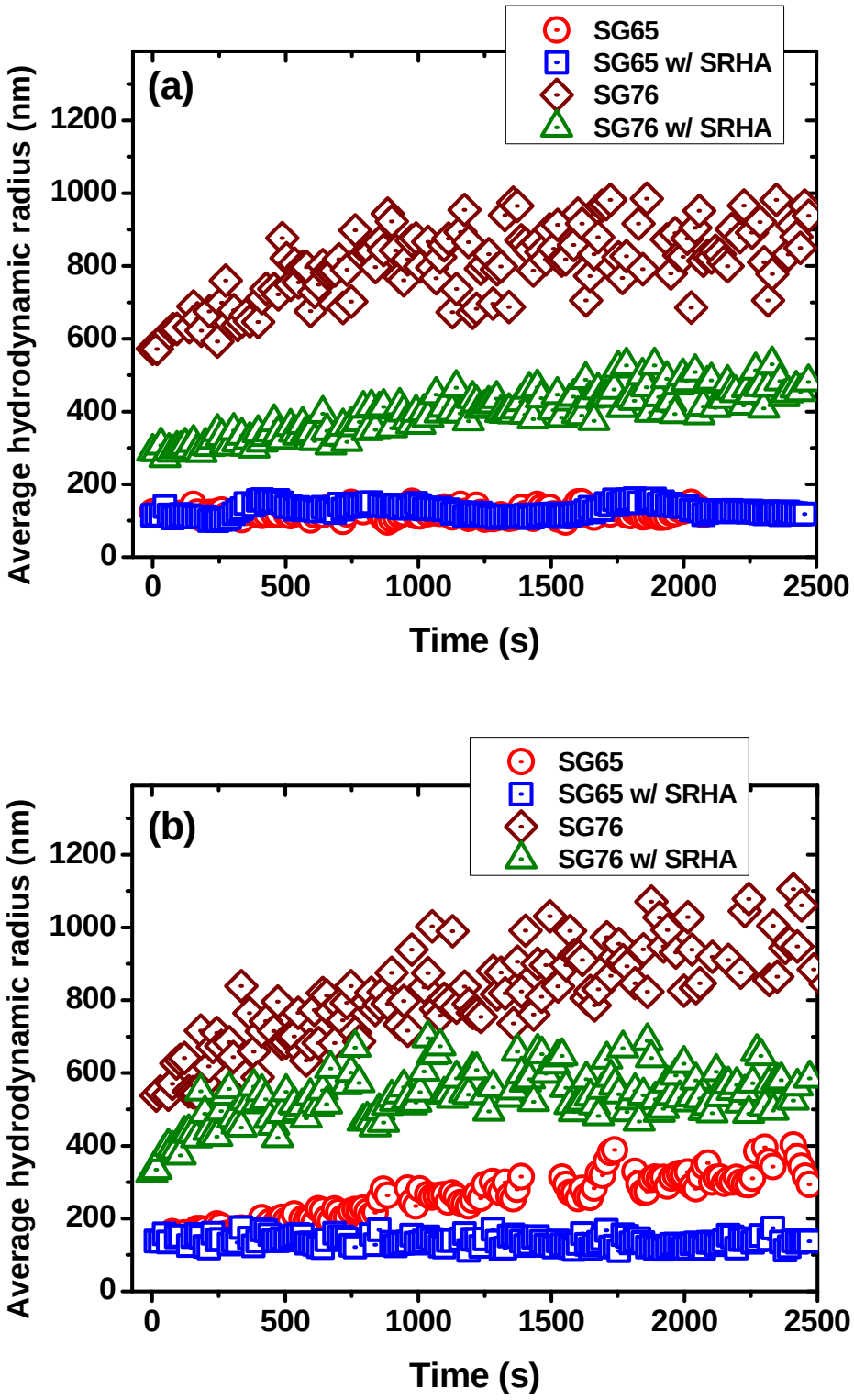

FIGURE S9: Aggregation profiles with (a) 10 mM NaCl and (b) 7 mM NaCl + 1 mM $CaCl_2$ in presence of 2.5 mg TOC/L SRHA.

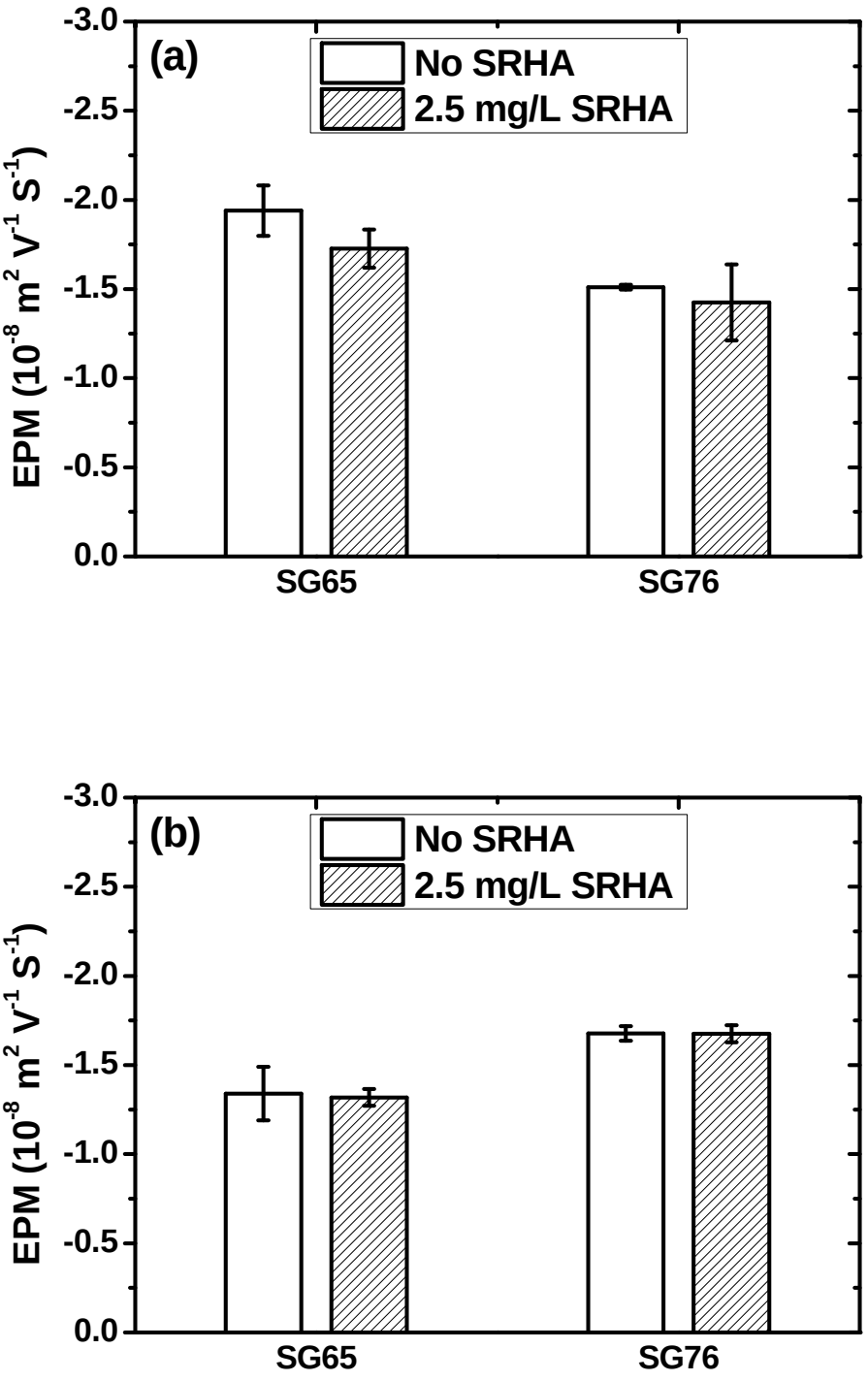

FIGURE S10. Electrophoretic mobility (EPM) of functionalized SWNTs under (a) 10 mM NaCl and (b) and 7 mM NaCl and 1 mM $CaCl_2$. Measurements were carried out at a pH of ~6.5 and a temperature of 20 °C.

Literature Cited

(1) Aich, N.; Flora, J. R. V.; Saleh, N. B. Preparation and characterization of stable aqueous higher-order fullerenes. *Nanotechnol* **2012**, *23*.

(2) Saleh, N. B.; Pfefferle, L. D.; Elimelech, M. Aggregation Kinetics of Multiwalled Carbon Nanotubes in Aquatic Systems: Measurements and Environmental Implications. *Environ Sci Technol* **2008**, *42*, 7963-7969.

(3) Saleh, N. B.; Pfefferle, L. D.; Elimelech, M. Influence of Biomacromolecules and Humic Acid on the Aggregation Kinetics of Single-Walled Carbon Nanotubes. *Environ Sci Technol* **2010**, *44*, 2412-2418.

(4) Humphrey, W.; Dalke, A.; Schulten, K. VMD: Visual molecular dynamics. *J. Molec. Graphics* **1996**, *14*, 33-38.

(5) Kästner, J.; Carr, J. M.; Keal, T. W.; Thiel, W.; Wander, A.; Sherwood, P. DL-FIND: An open-source geometry optimizer for atomistic simulations. *J. Phys. Chem. A* **2009**, *113*, 11856-11865.

(6) Grimme, S.; Antony, J.; Ehrlich, S.; Krieg, H. A consistent and accurate ab initio parametrization of density functional dispersion correction (DFT-D) for the 94 elements H-Pu. *J. Chem. Phys.* **2010**, *132*, 154104-154119.

(7) Grimme, S.; Ehrlich, S.; Goerigk, L. Effect of the damping function in dispersion corrected density functional theory. *J. Comput. Chem.* **2011**, *32*, 1456-1465.

(8) Ufimtsev, I. S.; Martinez, T. J. uantum chemistry on graphical processing units. 3. Analytical energy gradients, geometry optimization, and first principles molecular dynamics. *J. Chem. Theory Comput.* **2009**, *5*, 2619-2628.

(9) Bode, B. M.; Gordon, M. S. Macmolplt: a graphical user interface for GAMESS. *J. Mol. Graphics Mod.* **1998**, *16*, 133-138.